

# Charmonium dissociation in collisions with $\phi$ mesons in hadronic matter<sup>\*</sup>

Shi-Tao Ji(季石涛)<sup>1)</sup> Xiao-Ming Xu(许晓明)

Department of Physics, Shanghai University, Baoshan, Shanghai 200444, China

**Abstract:** The  $\phi$ -charmonium dissociation reactions in hadronic matter are studied. Unpolarised cross sections for  $\phi J/\psi \rightarrow D_s^- D_s^+$ ,  $\phi J/\psi \rightarrow D_s^{*-} D_s^+$  or  $D_s^- D_s^{*+}$ ,  $\phi J/\psi \rightarrow D_s^{*-} D_s^{*+}$ ,  $\phi \psi' \rightarrow D_s^- D_s^+$ ,  $\phi \psi' \rightarrow D_s^{*-} D_s^+$  or  $D_s^- D_s^{*+}$ ,  $\phi \psi' \rightarrow D_s^{*-} D_s^{*+}$ ,  $\phi \chi_c \rightarrow D_s^- D_s^+$ ,  $\phi \chi_c \rightarrow D_s^{*-} D_s^+$  or  $D_s^- D_s^{*+}$  and  $\phi \chi_c \rightarrow D_s^{*-} D_s^{*+}$  are calculated in the Born approximation, in the quark-interchange mechanism and with a temperature-dependent quark potential. The potential leads to remarkable temperature dependence of the cross sections. With the cross sections and the  $\phi$  distribution function we calculate the dissociation rates of the charmonia in interactions with the  $\phi$  meson in hadronic matter. The dependence of the rates on temperature and charmonium momentum is relevant to the influence of  $\phi$  mesons on charmonium suppression.

**Keywords:** charmonium dissociation cross sections, quark-interchange mechanism, dissociation rate

**PACS:** 25.75.-q, 24.85.+p, 12.38.Mh **DOI:** 10.1088/1674-1137/41/2/024101

## 1 Introduction

Hadronic matter affects the production of particles in relativistic heavy-ion collisions, and a change of  $J/\psi$  production in hadronic matter is appreciable. The change of  $J/\psi$  production is caused by inelastic meson-charmonium scattering [1–5] and spontaneous dissociation that may happen when the temperature is higher than the  $J/\psi$  dissociation temperature [6]. Studies of charmonium dissociation in collisions with hadrons are important in the field of relativistic heavy-ion collisions. Since  $\phi$ -meson production is enhanced in Au-Au collisions at Relativistic Heavy Ion Collider energies, it is interesting to investigate  $\phi$ -charmonium dissociation in hadronic matter. This is the subject of this paper.

We calculate  $\phi$ -charmonium dissociation cross sections in the Born approximation and in the quark-interchange mechanism [7]. The quark interchange mechanism between the incident meson and the charmonium breaks the charmonium and produces charmed mesons and/or charmed strange mesons. Dissociation of charmonia in collisions with  $\pi$ ,  $\rho$  and  $K$  in vacuum has been studied in Ref. [3] and dissociation in hadronic matter in Refs. [4, 5]. Meson-charmonium dissociation cross sections in hadronic matter differ from those in vacuum. The in-vacuum cross sections obtained in the quark-interchange approach are different from the cross sections obtained

in the meson-exchange approach [1] and in the short-distance approach [2]. The  $\phi$ -charmonium dissociation cross sections have not been calculated in the quark-interchange approach, the meson-exchange approach or the short-distance approach. In the present work we carry out the first calculation of the  $\phi$ -charmonium dissociation cross sections and find the temperature and energy dependence of the cross sections. The charmonium is not limited to  $J/\psi$  – it may be  $\psi'$  or  $\chi_c$ .

With the  $\phi$ -charmonium dissociation cross sections we calculate the dissociation rate of charmonium in interactions with the  $\phi$  meson in hadronic matter. The larger the dissociation rate is, the stronger charmonium suppression  $\phi$  mesons cause. From the dissociation rate we can understand the contribution of the  $\phi$  meson to charmonium suppression. Therefore, the second task of the paper is to calculate the dissociation rate. This is the first time the dissociation rate has been calculated, the temperature and charmonium-momentum dependence of the rate found and a conclusion drawn on the contribution of the  $\phi$  meson to charmonium suppression.

The remainder of this paper is organized as follows. In Section 2 formulas for the dissociation cross section and the dissociation rate are presented. In Section 3 we show numerical results of unpolarised  $\phi$ -charmonium dissociation cross sections and charmonium dissociation rates. Relevant discussions are given. A summary is given in Section 4.

Received 19 July 2016, Revised 9 October 2016

<sup>\*</sup> Supported by National Natural Science Foundation of China (11175111)

1) E-mail: 459756153@qq.com

©2017 Chinese Physical Society and the Institute of High Energy Physics of the Chinese Academy of Sciences and the Institute of Modern Physics of the Chinese Academy of Sciences and IOP Publishing Ltd

## 2 Cross-section and dissociation-rate formulas

The scattering  $A(s\bar{s}) + B(c\bar{c}) \rightarrow C(s\bar{c}) + D(c\bar{s})$  takes place due to quark interchange and interactions among the constituents (quarks and antiquarks). The scattering has two forms, the prior form and the post form. The scattering in the prior form means that gluon exchange occurs before quark interchange. The scattering in the post form contains gluon exchange after quark interchange. The scattering in the two forms is depicted in Figs. 1 and 2 in Ref. [5]. Cross-section formulas for the scattering are given in Refs. [4, 8]. Here we briefly introduce the formulas. Application of the cross section to get the charmonium dissociation rate follows.

We denote the spin, orbital angular momentum and four-momentum of meson  $i$  ( $i = s\bar{s}, c\bar{c}, s\bar{c}, c\bar{s}$ ) by  $S_i, L_i$  and  $P_i = (E_i, \vec{P}_i)$ , respectively. The Mandelstam variables are  $s = (E_{s\bar{s}} + E_{c\bar{c}})^2 - (\vec{P}_{s\bar{s}} + \vec{P}_{c\bar{c}})^2$  and  $t = (E_{s\bar{s}} - E_{s\bar{c}})^2 - (\vec{P}_{s\bar{s}} - \vec{P}_{s\bar{c}})^2$ . Let  $\vec{P}$  and  $\vec{P}'$  be the momenta of mesons  $A$  and  $C$  in the center-of-mass frame of  $A$  and  $B$ , respectively. The unpolarised cross section for the scattering in the prior form is

$$\begin{aligned} \sigma_{\text{prior}}^{\text{unpol}} &= \frac{1}{(2S_{s\bar{s}}+1)(2S_{c\bar{c}}+1)(2L_{c\bar{c}}+1)} \\ &\times \frac{1}{32\pi s} \frac{|\vec{P}'(\sqrt{s})|}{|\vec{P}(\sqrt{s})|} \sum_{SL_{c\bar{c}z}} (2S+1) \\ &\times \int_0^\pi d\theta |\mathcal{M}_{\text{fi}}^{\text{prior}}(s, t)|^2 \sin\theta, \end{aligned} \quad (1)$$

where  $\mathcal{M}_{\text{fi}}^{\text{prior}}$  is the transition amplitude for the scattering in the prior form,  $S$  is the total spin of mesons  $A$  and  $B$ ,  $L_{c\bar{c}z}$  is the magnetic projection quantum number of  $L_{c\bar{c}}$  and  $\theta$  is the angle between  $\vec{P}$  and  $\vec{P}'$ . The unpolarised cross section for the scattering in the post form is

$$\begin{aligned} \sigma_{\text{post}}^{\text{unpol}} &= \frac{1}{(2S_{s\bar{s}}+1)(2S_{c\bar{c}}+1)(2L_{c\bar{c}}+1)} \\ &\times \frac{1}{32\pi s} \frac{|\vec{P}'(\sqrt{s})|}{|\vec{P}(\sqrt{s})|} \sum_{SL_{c\bar{c}z}} (2S+1) \\ &\times \int_0^\pi d\theta |\mathcal{M}_{\text{fi}}^{\text{post}}(s, t)|^2 \sin\theta, \end{aligned} \quad (2)$$

where  $\mathcal{M}_{\text{fi}}^{\text{post}}$  is the transition amplitude for the scattering in the post form. The unpolarised cross section for  $A(s\bar{s}) + B(c\bar{c}) \rightarrow C(s\bar{c}) + D(c\bar{s})$  is

$$\sigma^{\text{unpol}} = \frac{1}{2} (\sigma_{\text{prior}}^{\text{unpol}} + \sigma_{\text{post}}^{\text{unpol}}). \quad (3)$$

Let  $\psi_{s\bar{s}} (\psi_{c\bar{c}}, \psi_{s\bar{c}}, \psi_{c\bar{s}})$  stand for the product of colour, spin, flavour and relative-motion wave functions of  $s\bar{s}$  ( $c\bar{c}$ ,

$s\bar{c}$ ,  $c\bar{s}$ ) and  $V_{ab}$  the interaction between constituents  $a$  and  $b$ . The transition amplitudes are given by

$$\begin{aligned} \mathcal{M}_{\text{fi}}^{\text{prior}} &= 4\sqrt{E_{s\bar{s}}E_{c\bar{c}}E_{s\bar{c}}E_{c\bar{s}}} \langle \psi_{s\bar{c}} | \langle \psi_{c\bar{s}} | \\ &\times (V_{s\bar{c}} + V_{c\bar{s}} + V_{sc} + V_{s\bar{c}}) | \psi_{s\bar{s}} \rangle | \psi_{c\bar{c}} \rangle, \end{aligned} \quad (4)$$

$$\begin{aligned} \mathcal{M}_{\text{fi}}^{\text{post}} &= 4\sqrt{E_{s\bar{s}}E_{c\bar{c}}E_{s\bar{c}}E_{c\bar{s}}} \langle \psi_{s\bar{c}} | \langle \psi_{c\bar{s}} | \\ &\times (V_{s\bar{s}} + V_{c\bar{c}} + V_{sc} + V_{s\bar{c}}) | \psi_{s\bar{s}} \rangle | \psi_{c\bar{c}} \rangle. \end{aligned} \quad (5)$$

The potential  $V_{ab}$  in coordinate space is

$$V_{ab}(\vec{r}) = V_{\text{si}}(\vec{r}) + V_{\text{ss}}(\vec{r}), \quad (6)$$

where  $\vec{r}$  is the relative coordinate of  $a$  and  $b$ ,  $V_{\text{si}}$  is the central spin-independent potential and  $V_{\text{ss}}$  the spin-spin interaction.  $V_{\text{si}}$  is given by [9]

$$\begin{aligned} V_{\text{si}}(\vec{r}) &= -\frac{\vec{\lambda}_a \cdot \vec{\lambda}_b}{2} \cdot \frac{3}{2} \frac{D}{4} \left[ 1.3 - \left( \frac{T}{T_c} \right)^4 \right] \tanh(Ar) \\ &+ \frac{\vec{\lambda}_a \cdot \vec{\lambda}_b}{2} \cdot \frac{6\pi}{25} \frac{v(\lambda r)}{r} \exp(-Er), \end{aligned} \quad (7)$$

where  $D = 0.7$  GeV,  $T_c = 0.175$  GeV,  $A = 1.5[0.75 + 0.25(T/T_c)^{10}]^6$  GeV,  $E = 0.6$  GeV and  $\lambda = \sqrt{3b_0/16\pi^2\alpha'}$  in which  $\alpha' = 1.04$  GeV<sup>-2</sup> and  $b_0 = 11 - \frac{2}{3}N_f$  with the quark flavour number  $N_f = 4$ .  $\vec{\lambda}_a \cdot \vec{\lambda}_b$  is the product of the Gell-Mann matrices for the colour generators of  $a$  and  $b$ . The dimensionless function  $v(x)$  is given by Buchmüller and Tye [10]. The short-distance part of  $V_{\text{si}}$  originates from one-gluon exchange plus perturbative one- and two-loop corrections. The intermediate-distance and large-distance part of  $V_{\text{si}}$  fits well the numerical potential obtained in the lattice gauge calculations [11]. At large distances  $V_{\text{si}}$  is independent of  $\vec{r}$  and exhibits a plateau. The plateau height decreases with increasing temperature. This means that confinement becomes weaker and weaker.

The spin-spin interaction with relativistic effects [7, 12] is [4, 13]

$$\begin{aligned} V_{\text{ss}}(\vec{r}) &= -\frac{\vec{\lambda}_a \cdot \vec{\lambda}_b}{2} \cdot \frac{16\pi^2}{25} \frac{d^3}{\pi^{3/2}} \exp(-d^2 r^2) \frac{\vec{s}_a \cdot \vec{s}_b}{m_a m_b} \\ &+ \frac{\vec{\lambda}_a \cdot \vec{\lambda}_b}{2} \cdot \frac{4\pi}{25} \frac{1}{r} \frac{d^2 v(\lambda r)}{dr^2} \frac{\vec{s}_a \cdot \vec{s}_b}{m_a m_b}, \end{aligned} \quad (8)$$

where  $\vec{s}_a$  ( $\vec{s}_b$ ) and  $m_a$  ( $m_b$ ) are the spin and mass of constituent  $a$  ( $b$ ), respectively. The flavour dependence of the interaction is relevant to quark masses as shown in  $\frac{1}{m_a m_b}$  and  $d$ ,

$$d^2 = \sigma_0^2 \left[ \frac{1}{2} + \frac{1}{2} \left( \frac{4m_a m_b}{(m_a + m_b)^2} \right)^4 \right] + \sigma_1^2 \left( \frac{2m_a m_b}{(m_a + m_b)} \right)^2, \quad (9)$$

where  $\sigma_0 = 0.15$  GeV and  $\sigma_1 = 0.705$ . The second term in Eq. (8) arises from the perturbative one- and two-loop corrections to the gluon propagator. The medium screening studied in lattice gauge theory at present affects only the central spin-independent potential. This allows us to keep using the spin-spin interaction relevant to perturbative QCD as done by Wong [6]. Therefore, the spin-spin interaction is independent of temperature.

By solving the Schrödinger equation with the central spin-independent potential plus the spin-spin interaction, meson masses and quark-antiquark relative-motion wave functions are obtained. In solving the Schrödinger equation the masses of the charm quark, the up quark and the strange quark are 1.51 GeV, 0.32 GeV and 0.5 GeV, respectively. The experimental masses of  $\phi$ ,  $J/\psi$ ,  $\psi'$ ,  $\chi_c$ ,  $D_s$  and  $D_s^*$  mesons [14] and the experimental data of  $S$ -wave  $I = 2$  elastic phase shifts for  $\pi\pi$  scattering in vacuum [15] are reproduced with  $V_{ab}(\vec{r})$  at  $T = 0$  and the quark-antiquark relative-motion wave functions.

When  $V_{ab}(\vec{r})$  and the quark-antiquark relative-motion wave functions obtained from the Schrödinger equation with the potential are used to calculate  $\mathcal{M}_{fi}^{\text{prior}}$  and  $\mathcal{M}_{fi}^{\text{post}}$ , we get  $\mathcal{M}_{fi}^{\text{prior}} = \mathcal{M}_{fi}^{\text{post}}$ . This is exactly what is concluded in Ref. [16] from a general argument.

With the unpolarised cross sections for charmonium dissociation we calculate the dissociation rate of charmonium in the interaction with the  $\phi$  meson in hadronic matter,

$$n\langle v_{\text{rel}}\sigma^{\text{unpol}}\rangle = \frac{3}{4\pi^2} \int_0^\infty \int_{-1}^1 d|\vec{k}| d\cos\theta \times \vec{k}^2 v_{\text{rel}} \sigma^{\text{unpol}} f(\vec{k}), \quad (10)$$

where  $n$  is the  $\phi$  number density,  $v_{\text{rel}}$  is the relative velocity of the  $\phi$  meson and the charmonium,  $\theta$  is the angle between the  $\phi$  momentum  $\vec{k}$  and the charmonium momentum and  $f(\vec{k})$  is the Bose-Einstein distribution that  $\phi$  mesons obey. The thermal average of  $v_{\text{rel}}\sigma^{\text{unpol}}$  is indicated by  $\langle v_{\text{rel}}\sigma^{\text{unpol}}\rangle$  [13]. The digit 3 in Eq. (10) is the spin degeneracy factor of the  $\phi$  meson. We denote by  $(|\vec{k}|, \theta, \varphi)$  the spherical polar coordinates of  $\vec{k}$  while the charmonium momentum is along the  $z$ -axis.  $\sigma^{\text{unpol}}$  is a function of  $\sqrt{s}$  and  $T$ .  $v_{\text{rel}}$  and  $\sqrt{s}$  are independent of the azimuth  $\varphi$ . The right-hand side of Eq. (10) is obtained from integration over  $\varphi$ . If  $f(\vec{k})$  is independent of  $\varphi$ , Eq. (10) is valid.

### 3 Numerical results and discussions

When a  $\phi$  meson collides with one of  $J/\psi$ ,  $\psi'$  and  $\chi_c$ ,  $D_s^-D_s^+$ ,  $D_s^*^-D_s^+$ ,  $D_s^-D_s^{*+}$  or  $D_s^*-D_s^{*+}$  is produced. Since the cross section for the production of  $D_s^*-D_s^+$  equals the cross section for the production of  $D_s^-D_s^{*+}$ , they are shown in the same figure. In Figs. 1–9 we plot cross sections for the following dissociation reac-

tions:  $\phi J/\psi \rightarrow D_s^-D_s^+$ ,  $\phi J/\psi \rightarrow D_s^*-D_s^+$  or  $D_s^-D_s^{*+}$ ,  $\phi J/\psi \rightarrow D_s^*-D_s^{*+}$ ,  $\phi\psi' \rightarrow D_s^-D_s^+$ ,  $\phi\psi' \rightarrow D_s^*-D_s^+$  or  $D_s^-D_s^{*+}$ ,  $\phi\psi' \rightarrow D_s^*-D_s^{*+}$ ,  $\phi\chi_c \rightarrow D_s^-D_s^+$ ,  $\phi\chi_c \rightarrow D_s^*-D_s^+$  or  $D_s^-D_s^{*+}$  and  $\phi\chi_c \rightarrow D_s^*-D_s^{*+}$ . Each curve in a figure corresponds to one of the six temperatures, 0,  $0.65T_c$ ,  $0.75T_c$ ,  $0.85T_c$ ,  $0.9T_c$  and  $0.95T_c$ .

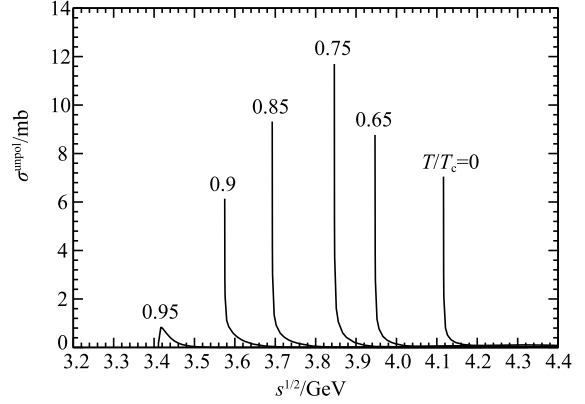


Fig. 1. Cross sections for  $\phi J/\psi \rightarrow D_s^-D_s^+$  at various temperatures.

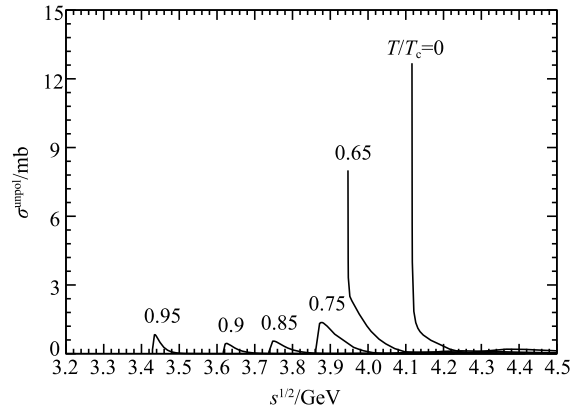


Fig. 2. Cross sections for  $\phi J/\psi \rightarrow D_s^*-D_s^+$  or  $D_s^-D_s^+$  at various temperatures.

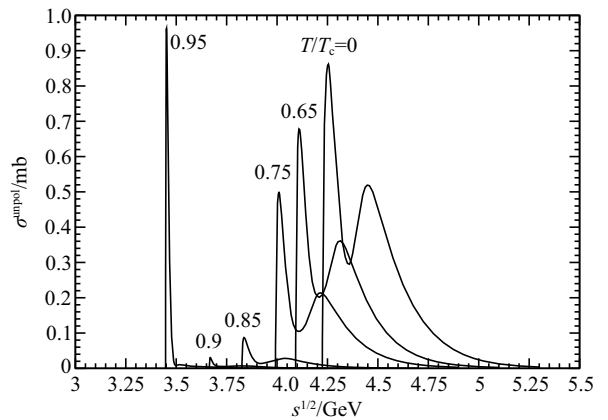


Fig. 3. Cross sections for  $\phi J/\psi \rightarrow D_s^*-D_s^+$  at various temperatures.

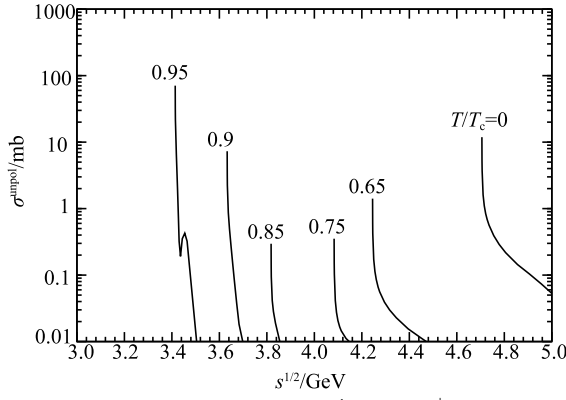


Fig. 4. Cross sections for  $\phi\psi' \rightarrow D_s^- D_s^+$  at various temperatures.

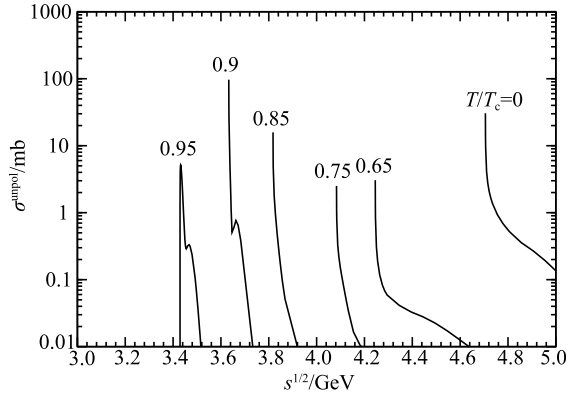


Fig. 5. Cross sections for  $\phi\psi' \rightarrow D_s^{*-} D_s^+$  or  $D_s^- D_s^{*+}$  at various temperatures.

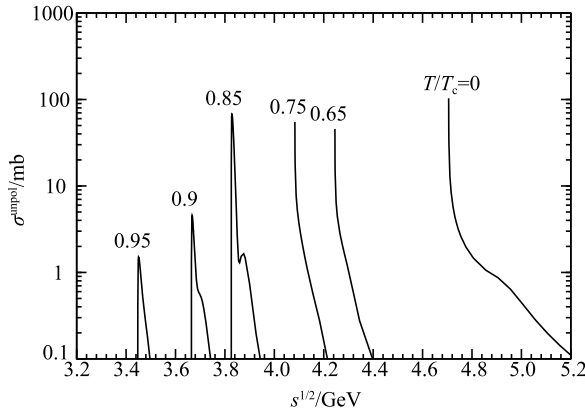


Fig. 6. Cross sections for  $\phi\psi' \rightarrow D_s^{*-} D_s^{*+}$  at various temperatures.

Let  $m_{s\bar{s}}$ ,  $m_{c\bar{c}}$ ,  $m_{s\bar{c}}$  and  $m_{c\bar{s}}$  be the masses of  $s\bar{s}$ ,  $c\bar{c}$ ,  $s\bar{c}$  and  $c\bar{s}$  mesons, respectively. The absolute value of  $\vec{P}$  in Eqs. (1) and (2) is  $|\vec{P}| = \frac{1}{2} \sqrt{[s - (m_{s\bar{s}} + m_{c\bar{c}})^2][s - (m_{s\bar{s}} - m_{c\bar{c}})^2]}/s$ . At the threshold of exothermic reactions  $\sqrt{s} = m_{s\bar{s}} + m_{c\bar{c}}$ ,  $|\vec{P}| = 0$ ,  $\sigma_{\text{prior}}^{\text{unpol}} = \infty$ ,  $\sigma_{\text{post}}^{\text{unpol}} = \infty$  and  $\sigma^{\text{unpol}} = \infty$ . For example, in Fig. 1 the cross sections for the exothermic reactions at

$T/T_c = 0, 0.65, 0.75, 0.85$  and  $0.9$  diverge at the threshold energies. Since the infinite values cannot be plotted, we start plotting the cross sections at  $\sqrt{s} = m_{s\bar{s}} + m_{c\bar{c}} + 10^{-4}$  GeV. The threshold energy for the endothermic reaction is  $m_{s\bar{c}} + m_{c\bar{s}}$  and the corresponding  $|\vec{P}|$  does not equal 0. Hence, the cross section for the endothermic reaction does not diverge and instead has one peak at  $T/T_c = 0.95$ , which takes the value  $0.823$  mb at  $\sqrt{s} = 3.418$  GeV.

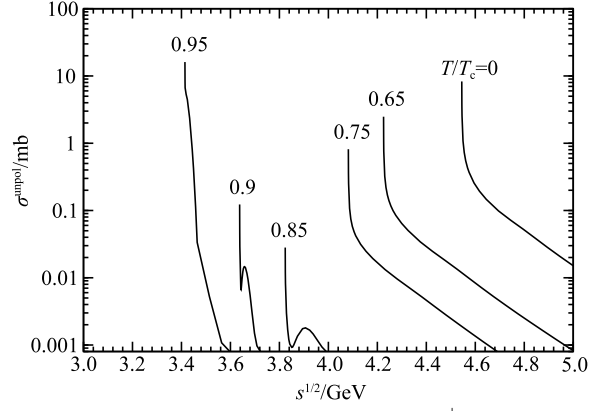


Fig. 7. Cross sections for  $\phi\chi_c \rightarrow D_s^- D_s^+$  at various temperatures.

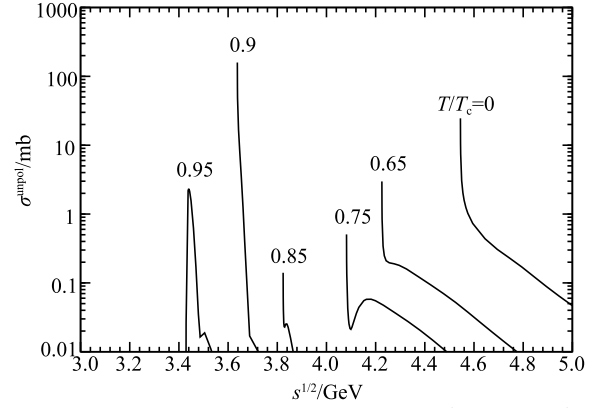


Fig. 8. Cross sections for  $\phi\chi_c \rightarrow D_s^{*-} D_s^+$  or  $D_s^- D_s^{*+}$  at various temperatures.

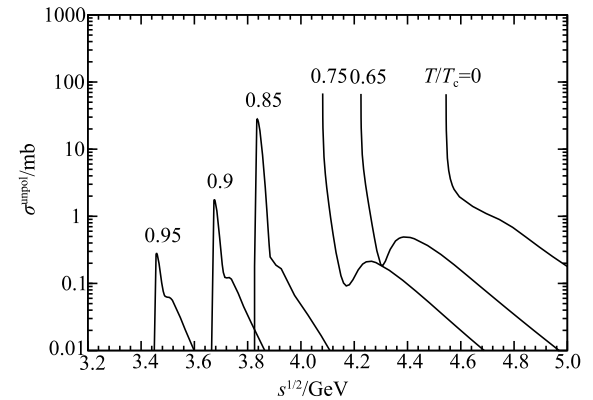


Fig. 9. Cross sections for  $\phi\chi_c \rightarrow D_s^{*-} D_s^{*+}$  at various temperatures.

We take Fig. 8 to account for the peak structure appearing in the cross-section curves. Generally, only a small number of partial waves contribute to low-energy reactions. Around the main peak near the threshold energy at  $T/T_c = 0.95$ , the  $s$  waves of the scattering constituents (quarks and/or antiquarks) contribute to the cross section. For  $\sqrt{s}$  away from the threshold energy,  $p$  waves make a contribution to the cross section and form the small peak beside the main peak. The contributions of  $s$  and  $p$  waves affect  $|\mathcal{M}_{\text{fi}}^{\text{prior}}|^2$  in Eq. (1) and  $|\mathcal{M}_{\text{fi}}^{\text{post}}|^2$  in Eq. (2). As  $\sqrt{s}$  increases from the threshold energy,  $|\mathcal{M}_{\text{fi}}^{\text{prior}}|^2$  and  $|\mathcal{M}_{\text{fi}}^{\text{post}}|^2$  increase first and then decrease, which comes from the  $s$ -wave contribution; when  $\sqrt{s}$  increases further,  $|\mathcal{M}_{\text{fi}}^{\text{prior}}|^2$  and  $|\mathcal{M}_{\text{fi}}^{\text{post}}|^2$  increase again and then decrease, which originates from the  $p$ -wave contribution. For any endothermic reaction the factor  $\frac{1}{s} \frac{|\vec{P}'|}{|\vec{P}|}$  increases first and then decreases when  $\sqrt{s}$  increases from the threshold energy. Therefore, we can see one or more peaks in the cross-section curves for the endothermic reaction. For any exothermic reaction the factor  $\frac{1}{s} \frac{|\vec{P}'|}{|\vec{P}|}$  decreases monotonically. If the factor decreases very fast and  $|\mathcal{M}_{\text{fi}}^{\text{prior}}|^2 + |\mathcal{M}_{\text{fi}}^{\text{post}}|^2$  increases slowly, no peaks appear, as shown by the curve at  $T = 0$ . If the factor decreases slowly and  $|\mathcal{M}_{\text{fi}}^{\text{prior}}|^2 + |\mathcal{M}_{\text{fi}}^{\text{post}}|^2$  increases fast, one peak appears as shown by the curve at  $T/T_c = 0.75$ . Whether a peak appears depends on the decrease of the factor and the increase of  $|\mathcal{M}_{\text{fi}}^{\text{prior}}|^2 + |\mathcal{M}_{\text{fi}}^{\text{post}}|^2$ .

Cross sections for  $A + B \rightarrow C + D$  depend on the masses of mesons  $A$ ,  $B$ ,  $C$  and  $D$ . When the temperature approaches the critical temperature  $T_c$ ,  $D_s^\pm$  and  $D_s^{*\pm}$  become degenerate in mass. The sum of the  $D_s^-$  and  $D_s^+$  masses almost equals the sum of the  $D_s^{*-}$  and  $D_s^{*+}$  masses or the sum of the  $D_s^{*-}$  and  $D_s^{*+}$  masses at  $T = 0.95T_c$ . However, the cross sections for  $\phi J/\psi \rightarrow D_s^- D_s^+$ ,  $\phi J/\psi \rightarrow D_s^{*-} D_s^{*+}$  and  $\phi J/\psi \rightarrow D_s^{*-} D_s^{*+}$  are still different, as shown in Figs. 1–3. This is because the spin matrix elements involved in the transition amplitude are different for the three reactions.

The two reactions  $\phi J/\psi \rightarrow D_s^{*-} D_s^{*+}$  and  $\phi J/\psi \rightarrow D_s^{*-} D_s^{*+}$  are endothermic at  $T/T_c = 0.75$ ,  $0.85$  and  $0.9$ . The sum of the  $D_s^{*-}$  and  $D_s^{*+}$  masses is smaller than the sum of the  $D_s^{*-}$  and  $D_s^{*+}$  masses. The square root of the Mandelstam variable  $\sqrt{s_{\text{pa}}}$  corresponding to the peak cross section of  $\phi J/\psi \rightarrow D_s^{*-} D_s^{*+}$  is smaller than  $\sqrt{s_{\text{paa}}}$  corresponding to the peak cross section of  $\phi J/\psi \rightarrow D_s^{*-} D_s^{*+}$ . The  $\phi$  momentum  $\vec{P}$  of  $\phi J/\psi \rightarrow D_s^{*-} D_s^{*+}$  at  $\sqrt{s_{\text{pa}}}$  has a magnitude smaller than the one of  $\phi J/\psi \rightarrow D_s^{*-} D_s^{*+}$  at  $\sqrt{s_{\text{paa}}}$ . Accordingly, the factor  $\frac{1}{s} \frac{|\vec{P}'|}{|\vec{P}|}$  in Eqs. (1) and (2) is larger for  $\phi J/\psi \rightarrow D_s^{*-} D_s^{*+}$  than for  $\phi J/\psi \rightarrow D_s^{*-} D_s^{*+}$ . On the other hand, the rela-

tive momentum  $\vec{p}_{\text{ab}}$  of constituents  $a$  and  $b$  due to small  $|\vec{P}|$  in  $\phi J/\psi \rightarrow D_s^{*-} D_s^{*+}$  has a magnitude smaller than that in  $\phi J/\psi \rightarrow D_s^{*-} D_s^{*+}$ . The mesonic quark-antiquark relative-motion wave function  $\psi_{\text{ab}}(\vec{p}_{\text{ab}})$  in the transition amplitude for  $\phi J/\psi \rightarrow D_s^{*-} D_s^{*+}$  is larger than the wave function for  $\phi J/\psi \rightarrow D_s^{*-} D_s^{*+}$ . Therefore, the peak cross section of  $\phi J/\psi \rightarrow D_s^{*-} D_s^{*+}$  is larger than the peak cross section of  $\phi J/\psi \rightarrow D_s^{*-} D_s^{*+}$  at  $T/T_c = 0.75$ ,  $0.85$  and  $0.9$  as seen in Figs. 2 and 3.

The reactions  $\phi \psi' \rightarrow D_s^- D_s^+$  and  $\phi \chi_c \rightarrow D_s^- D_s^+$  are exothermic below  $T_c$ . The reactions  $\phi J/\psi \rightarrow D_s^- D_s^+$ ,  $\phi \psi' \rightarrow D_s^{*-} D_s^{*+}$  and  $\phi \chi_c \rightarrow D_s^{*-} D_s^{*+}$  are exothermic below  $0.95T_c$ . The threshold energy of every exothermic reaction is  $m_\phi + m_{c\bar{c}}$ , where  $m_\phi$  and  $m_{c\bar{c}}$  are the  $\phi$  mass and the charmonium mass, respectively. We start calculating cross sections for exothermic reactions at  $\sqrt{s} = m_\phi + m_{c\bar{c}} + 10^{-4}$  GeV and the cross sections at the energies correspond to the curve tops. Exothermic reactions take place as long as the two initial mesons overlap and even though the two initial mesons are at rest. However, the sizes of the initial and final mesons affect the cross sections. In  $\phi J/\psi \rightarrow D_s^- D_s^+$  the sizes of  $J/\psi$ ,  $D_s^-$  and  $D_s^+$  mesons at  $T/T_c = 0$ ,  $0.65$  and  $0.75$  are so small that the influence of confinement is small at such sizes. The increase of the  $J/\psi$  size with increasing temperature causes the cross section at  $m_\phi + m_{J/\psi} + 10^{-4}$  GeV to increase. From  $T/T_c = 0.75$  to  $0.9$  the  $D_s^-$  ( $D_s^+$ ) size increases quickly and confinement becomes important. Since the plateau of  $V_{\text{si}}(\vec{r})$  at large distances lowers with increasing temperature, confinement of the quark and the antiquark to form  $D_s^-$  and  $D_s^+$  mesons becomes weaker and weaker and at  $m_\phi + m_{J/\psi} + 10^{-4}$  GeV the cross section thus decreases. In the  $\phi \psi'$  and  $\phi \chi_c$  reactions the sizes of  $\phi$ ,  $\psi'$  and  $\chi_c$  mesons are not small and the influence of confinement on combining a quark and an antiquark to form a  $D_s^-$ ,  $D_s^+$ ,  $D_s^{*-}$  or  $D_s^{*+}$  meson is appreciable at such sizes. Weakening confinement reduces cross sections with increasing temperature. When the temperature increases from  $T/T_c = 0.75$  to  $0.9$ , the  $\phi$ ,  $\psi'$  and  $\chi_c$  sizes increase rapidly and cross sections can thus go up. The two factors make the cross section for each of the four  $\phi \psi'$  or  $\phi \chi_c$  reaction channels at the threshold energy plus  $10^{-4}$  GeV decrease first and increase next, as shown in Figs. 4, 5, 7 and 8, while temperature the changes from  $0$  to  $0.9T_c$ .

The  $\phi$  meson consists of the strange quark and the strange antiquark, but the  $\pi$  meson does not. It is thus interesting to compare the  $\phi$ -charmonium dissociation cross sections with  $\pi$ -charmonium dissociation cross sections. The temperature-dependent cross sections for charmonium dissociation in collision with  $\pi$  have been obtained in Ref. [4] with the quark-interchange mechanism. Since the  $\pi$  meson is a pseudoscalar meson, the  $\pi$ -induced charmonium dissociation has three channels,

$\pi + \text{charmonium} \rightarrow \bar{D}^* + D$ ,  $\pi + \text{charmonium} \rightarrow \bar{D} + D^*$  and  $\pi + \text{charmonium} \rightarrow \bar{D}^* + D^*$ . These reactions are all endothermic. Since the  $\phi$  meson is a vector meson, the  $\phi$ -induced charmonium dissociation has four channels,  $\phi + \text{charmonium} \rightarrow D_s^- + D_s^+$ ,  $\phi + \text{charmonium} \rightarrow D_s^{*-} + D_s^+$ ,  $\phi + \text{charmonium} \rightarrow D_s^- + D_s^{*+}$  and  $\phi + \text{charmonium} \rightarrow D_s^{*-} + D_s^{*+}$ . Each of the  $\phi + \text{charmonium}$  reactions in Figs. 1, 2 and 4-9 is exothermic when the temperature is smaller than a particular value. At a given temperature the peak cross section of a  $\pi + \text{charmonium}$  channel is either larger or smaller than the one of a  $\phi + \text{charmonium}$  channel if it is endothermic. Remarkable temperature dependence has been shown by the  $\pi$ -charmonium dissociation cross sections and the  $\phi$ -charmonium dissociation cross sections.

Charmonium dissociation in collision with the  $\phi$  meson has four channels. The unpolarised dissociation cross section in the dissociation-rate formula is the sum of the unpolarised cross sections for the four channels. In collision of  $\phi$  with  $J/\psi$  ( $\psi'$ ,  $\chi_c$ )  $\sigma^{\text{unpol}}$  is the unpolarised cross section for  $\phi J/\psi \rightarrow D_s^- D_s^+ + D_s^{*-} D_s^+ + D_s^- D_s^{*+} + D_s^{*-} D_s^{*+}$  ( $\phi \psi' \rightarrow D_s^- D_s^+ + D_s^{*-} D_s^+ + D_s^- D_s^{*+} + D_s^{*-} D_s^{*+}$ ,  $\phi \chi_c \rightarrow D_s^- D_s^+ + D_s^{*-} D_s^+ + D_s^- D_s^{*+} + D_s^{*-} D_s^{*+}$ ).

Numerical results of dissociation rates as functions of charmonium momentum are plotted in Figs. 10-12. Since the  $\phi$  distribution function, the unpolarised cross section and the relative velocity in Eq. (10) vary with temperature, the dissociation rate depends on the temperature. As the temperature increases from  $T/T_c = 0.65$  to 0.95, the  $\phi$  mass decreases and the  $\phi$  distribution function increases. This is a factor that increases the charmonium dissociation rate. At zero charmonium momentum the slope of each curve is zero. Because  $\phi$  mesons obey the Bose-Einstein distribution, there is a domain of  $k$  in Eq. (10), which keeps  $\sqrt{s}$  near the threshold energy so that the unpolarised cross section contributes significantly. While the charmonium momentum increases, the domain shrinks and the dissociation rate thus decreases. Since the dissociation rates of  $J/\psi$ ,  $\psi'$

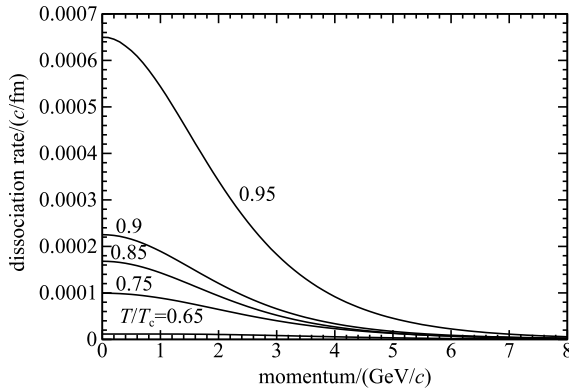


Fig. 10. Dissociation rate of  $J/\psi$  with  $\phi$  versus the  $J/\psi$  momentum at various temperatures.

and  $\chi_c$  with  $\phi$  are less than 0.00066, 0.002 and 0.0008, respectively, the charmonium suppression caused by the  $\phi$ -charmonium dissociation is weak.

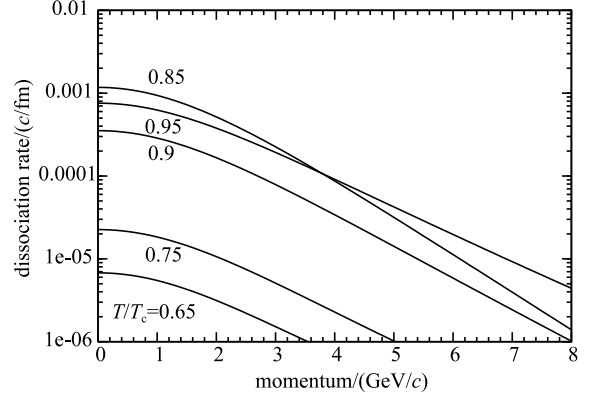


Fig. 11. Dissociation rate of  $\psi'$  with  $\phi$  versus the  $\psi'$  momentum at various temperatures.

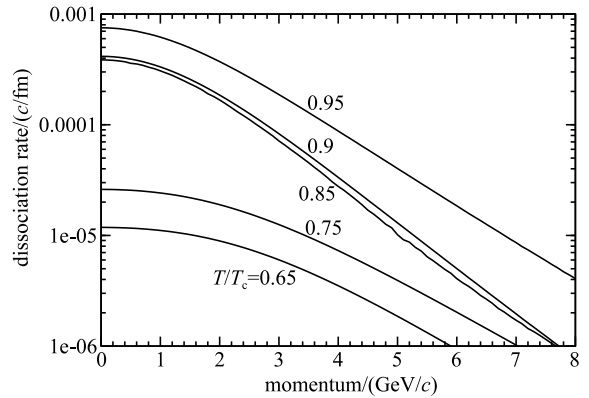


Fig. 12. Dissociation rate of  $\chi_c$  with  $\phi$  versus the  $\chi_c$  momentum at various temperatures.

## 4 Summary

Using the temperature-dependent quark potential that is derived from perturbative QCD at short distances and the lattice gauge results at intermediate- and large-distances, we obtain the unpolarised cross sections in the quark-interchange mechanism and in the Born approximation. The reactions that we concern are  $\phi J/\psi \rightarrow D_s^- D_s^+$ ,  $\phi J/\psi \rightarrow D_s^{*-} D_s^+$  or  $D_s^- D_s^{*+}$ ,  $\phi J/\psi \rightarrow D_s^{*-} D_s^{*+}$ ,  $\phi \psi' \rightarrow D_s^- D_s^+$ ,  $\phi \psi' \rightarrow D_s^{*-} D_s^+$  or  $D_s^- D_s^{*+}$ ,  $\phi \psi' \rightarrow D_s^{*-} D_s^{*+}$ ,  $\phi \chi_c \rightarrow D_s^- D_s^+$ ,  $\phi \chi_c \rightarrow D_s^{*-} D_s^+$  or  $D_s^- D_s^{*+}$  and  $\phi \chi_c \rightarrow D_s^{*-} D_s^{*+}$ . The meson masses, confinement and mesonic quark-antiquark relative-motion wave functions cause the large variation of the cross sections with respect to temperature. Medium effects on the dissociation reactions are prominent. When the confinement gives similar contributions to two reaction channels, the spin-spin interaction causes a difference

in the unpolarised cross sections for the two channels. Using the unpolarised cross sections for the 12 reactions, we obtain the dissociation rates of charmonia in the inter-

actions with the  $\phi$  meson. The rates generally increase with increasing temperature or decrease with increasing charmonium momentum. The rates are quite small.

## References

- 1 S. G. Matinyan and B. Müller, *Phys. Rev. C*, **58**: 2994 (1998); K. L. Haglin, *Phys. Rev. C*, **61**: 031902 (2000); K. L. Haglin and C. Gale, *Phys. Rev. C*, **63**: 065201 (2001); Z. Lin and C. M. Ko, *Phys. Rev. C*, **62**: 034903 (2000); J. Phys. G, **27**: 617 (2001); Y. S. Oh, T. S. Song, and S. H. Lee, *Phys. Rev. C*, **63**: 034901 (2001); F. S. Navarra, M. Nielsen, and M. R. Robilotta, *Phys. Rev. C*, **64**: 021901(R) (2001); L. Maiani, F. Piccinini, A. D. Polosa, and V. Riquer, *Nucl. Phys. A*, **741**: 273 (2004); A. Bourque and C. Gale, *Phys. Rev. C*, **78**: 035206 (2008); *Phys. Rev. C*, **80**: 015204 (2009)
- 2 M. E. Peskin, *Nucl. Phys. B*, **156**: 365 (1979); G. Bhanot and M. E. Peskin, *Nucl. Phys. B*, **156**: 391 (1979); D. Kharzeev and H. Satz, *Phys. Lett. B*, **334**: 155 (1994); F. Arleo, P. B. Gosiaux, T. Gousset, and J. Aichelin, *Phys. Rev. D*, **65**: 014005 (2001)
- 3 K. Martins, D. Blaschke, and E. Quack, *Phys. Rev. C*, **51**: 2723 (1995); C. Y. Wong, E. S. Swanson, and T. Barnes, *Phys. Rev. C*, **62**: 045201 (2000); *Phys. Rev. C*, **65**: 014903 (2001); T. Barnes, E. S. Swanson, C. Y. Wong, and X. M. Xu, *Phys. Rev. C*, **68**: 014903 (2003); J. P. Hilbert, N. Black, T. Barnes, and E. S. Swanson, *Phys. Rev. C*, **75**: 064907 (2007)
- 4 J. Zhou and X. M. Xu, *Phys. Rev. C*, **85**: 064904 (2012)
- 5 S. T. Ji, Z. Y. Shen, and X. M. Xu, *J. Phys. G*, **42**: 095110 (2015)
- 6 C. Y. Wong, *Phys. Rev. C*, **65**: 034902 (2002)
- 7 T. Barnes and E. S. Swanson, *Phys. Rev. D*, **46**: 131 (1992); E. S. Swanson, *Ann. Phys. (N.Y.)*, **220**: 73 (1992)
- 8 Y. Q. Li and X. M. Xu, *Nucl. Phys. A*, **794**: 210 (2007)
- 9 Y. P. Zhang, X. M. Xu, and H. J. Ge, *Nucl. Phys. A*, **832**: 112 (2010)
- 10 W. Buchmüller and S. H. H. Tye, *Phys. Rev. D*, **24**: 132 (1981)
- 11 F. Karsch, E. Laermann, and A. Peikert, *Nucl. Phys. B*, **605**: 579 (2001)
- 12 S. Godfrey and N. Isgur, *Phys. Rev. D*, **32**: 189 (1985)
- 13 X. M. Xu, *Nucl. Phys. A*, **697**: 825 (2002)
- 14 K. A. Olive et al, Particle Data Group, *Chin. Phys. C*, **38**: 090001 (2014)
- 15 E. Colton et al, *Phys. Rev. D*, **3**: 2028 (1971); N. B. Durusoy et al, *Phys. Lett. B*, **45**: 517 (1973); W. Hoogland et al, *Nucl. Phys. B*, **126**: 109 (1977); M. J. Losty et al, *Nucl. Phys. B*, **69**: 185 (1974)
- 16 N. F. Mott and H. S. W. Massey, *The Theory of Atomic Collisions* (Oxford: Clarendon Press, 1965); T. Barnes, N. Black, and E. S. Swanson, *Phys. Rev. C*, **63**: 025204 (2001); C. Y. Wong and H. W. Crater, *Phys. Rev. C*, **63**: 044907 (2001)